Photonic-plasmonic hybrid microcavities: Physics and applications

Hongyu Zhang(张红钰), Wen Zhao(赵闻), Yaotian Liu(刘耀天), Jiali Chen(陈佳丽), Xinyue Wang(王欣月), and Cuicui Lu(路翠翠)

Citation: Chin. Phys. B, 2021, 30 (**11**): 117801. DOI: 10.1088/1674-1056/ac0db3
Journal homepage: http://cpb.iphy.ac.cn; http://iopscience.iop.org/cpb

What follows is a list of articles you may be interested in

Topology optimization method of metamaterials design for efficient enhanced transmission through arbitrary-shaped sub-wavelength aperture

Pengfei Shi(史鹏飞), Yangyang Cao(曹阳阳), Hongge Zhao(赵宏革), Renjing Gao(高仁璟), and Shutian Liu(刘书田)
Chin. Phys. B, 2021, 30 (**9**): 097806. DOI: 10.1088/1674-1056/ac0cde

Real-time quantitative optical method to study temperature dependence of crack propagation process in colloidal photonic crystal film

Lin Dong-Feng, Xu Yu-Zhuan, Shi Jiang-Jian, Zhang Yu, Luo Yan-Hong, Li Dong-Mei, Meng Qing-Bo
Chin. Phys. B, 2015, 24 (**7**): 077803. DOI: 10.1088/1674-1056/24/7/077803

Giant enhancement of Kerr rotation in two-dimensional Bismuth iron garnet/Ag photonic crystals

Liang Hong, Liu Huan, Zhang Qiang, Fu Shu-Fang, Zhou Sheng, Wang Xuan-Zhang
Chin. Phys. B, 2015, 24 (**6**): 067807. DOI: 10.1088/1674-1056/24/6/067807

Polarization characteristics of chiral photonic crystal fibers with an elliptical hollow core

Li She, Li Jun-Qing, Cao Yu-Sheng
Chin. Phys. B, 2013, 22 (**11**): 117806. DOI: 10.1088/1674-1056/22/11/117806

Tunneling effect in cavity-resonator-coupled arrays

Ma Hua, Qu Shao-Bo, Liang Chang-Hong, Zhang Jie-Qiu, Xu Zhuo, Wang Jia-Fu
Chin. Phys. B, 2013, 22 (**5**): 057805. DOI: 10.1088/1674-1056/22/5/057805

TOPICAL REVIEW — Optical field manipulation

Photonic-plasmonic hybrid microcavities: Physics and applications*

Hongyu Zhang(张红钰)[1], Wen Zhao(赵闻)[1,3], Yaotian Liu(刘耀天)[1], Jiali Chen(陈佳丽)[1], Xinyue Wang(王欣月)[1], and Cuicui Lu(路翠翠)[1,2,†]

[1] *Key Laboratory of Advanced Optoelectronic Quantum Architecture and Measurements of Ministry of Education, Beijing Key Laboratory of Nanophotonics and Ultrafine Optoelectronic Systems, School of Physics, Beijing Institute of Technology, Beijing* 100081, *China*
[2] *Collaborative Innovation Center of Light Manipulations and Applications, Shandong Normal University, Jinan* 250358, *China*
[3] *School of Physical Engineering, Qufu Normal University, Qufu* 273165, *China*

(Received 27 April 2021; revised manuscript received 21 June 2021; accepted manuscript online 23 June 2021)

Photonic-plasmonic hybrid microcavities, which possess a higher figure of merit Q/V (the ratio of quality factor to mode volume) than that of pure photonic microcavities or pure plasmonic nano-antennas, play key roles in enhancing light–matter interaction. In this review, we summarize the typical photonic-plasmonic hybrid microcavities, such as photonic crystal microcavities combined with plasmonic nano-antenna, whispering gallery mode microcavities combined with plasmonic nano-antenna, and Fabry–Perot microcavities with plasmonic nano-antenna. The physics and applications of each hybrid photonic-plasmonic system are illustrated. The recent developments of topological photonic crystal microcavities and topological hybrid nano-cavities are also introduced, which demonstrates that topological microcavities can provide a robust platform for the realization of nanophotonic devices. This review can bring comprehensive physical insights of the hybrid system, and reveal that the hybrid system is a good platform for realizing strong light–matter interaction.

Keywords: hybrid microcavities, photonic crystal, plasmonic nano-antenna, figure of merit Q/V

PACS: 78.67.Pt, 42.70.Qs, 42.55.Sa, 61.46.Bc **DOI:** 10.1088/1674-1056/ac0db3

1. Introduction

Optical microcavities are essential platform for enhancing light–matter interaction, which have wide applications in biosensing,[1–5] optical trapping,[6–9] cavity quantum electrodynamics (QED),[10–15] on-chip nano-lasers[16–20] and surface-enhanced Raman scattering (SERS).[21–24] The quality factor Q and mode volume V represent the spectral energy density and spatial energy density of the optical microcavities, and they quantitatively describe how long in time the cavity can store light and how small in space the cavity can localize light.[25–30] The light–matter interaction strength is proportional to Q^m/V^n for many processes (where m and n are positive integers or fractions in general), so the figure of merit Q/V is introduced as a basic index to evaluate the ability of optical microcavities in enhancing light–matter interaction.[25,26] How to achieve high Q/V optical microcavities for strong light–matter interaction is the core task. In the last decade, great progress has been made in realizing high quality factor Q dielectric microcavities for improving the value of Q/V, such as whispering-gallery-mode (WGM) microcavities[31–40] and photonic crystal (PhC) cavities.[26,41–47] However, the mode volume V in these systems is always larger than $(\lambda/2)^3$ due to the laws of diffraction, which limits the improvement of the figure of merit Q/V.[33–36,42–45]

On the other hand, plasmonic nano-cavities or plasmonic nano-antennas have the properties of localized surface plasmon resonances, so they can confine light into ultra-small volumes far below the diffraction limit. The high value of Q/V can be realized due to the ultra-small mode volume V.[48–55] However, the quality factor Q in plasmonic systems is typically below 50 due to serious absorption and scattering losses.[56–59] The enhancement of the figure of merit Q/V is still limited. There is hence a strong need for a constructive route toward resonators that leverage plasmonic nano-antennas for ultratight confinement, yet operate at desirable Q.

Photonic-plasmonic hybrid microcavities have been proposed to access the regime of deep subwavelength confinement, owing to their plasmonic constituents, while at the same time inheriting larger quality factor benefiting from a dielectric microcavity characteristic.[60–68] Several groups have explored the hybrid systems by embedding single metal nano-particles or plasmonic nanoantennas into dielectric microcavities, such as PhC nano-cavities[43–45,65] and WGM microcavities.[60] The calculated results in previous reports indicate that the strength of light–matter interaction in hybrid systems is stronger than the individual constituents, and the successful fabrication of the hybrid structure in experiments makes the hybrid systems get more attention for applications in enhancing light–matter interaction.[66,67,69]

*Project supported by the National Natural Science Foundation of China (Grant Nos. 91850117 and 11654003) and Beijing Institute of Technology Research Fund Program for Young Scholars.

†Corresponding author. E-mail: cuicuilu@bit.edu.cn

Taking three types of typical hybrid microcavities as examples, which refer to hybrid microcavities based on PhC microcavities,[65,67,69–72] hybrid microcavities based on WGM microcavities[60,62,66,73] and hybrid microcavities based on F-P microcavities,[63,68] we summarize a brief history of their respective development. As is shown in Fig. 1, the first hybrid microcavity was proposed and fabricated by Barth *et al.* in 2010, which consists of a two-dimensional (2D) PhC microcavity and metal nanoparticles.[67] It opened new routes for controlling light–matter interaction at the nanoscale. During the next decade, hybrid microcavities based on PhC microcavities were developed toward miniaturization. The hybrid microcavities consist of one-dimensional (1D) PhC microcavities and plasmonic nano-antennas have also been realized.[69,71,72] The applications of hybrid microcavities based on PhC microcavities in fundamental quantum optics began to be studied in 2019.[72] Strong coupling was realized in hybrid photonic-plasmonic nano-cavity in 2020,[65] which indicates

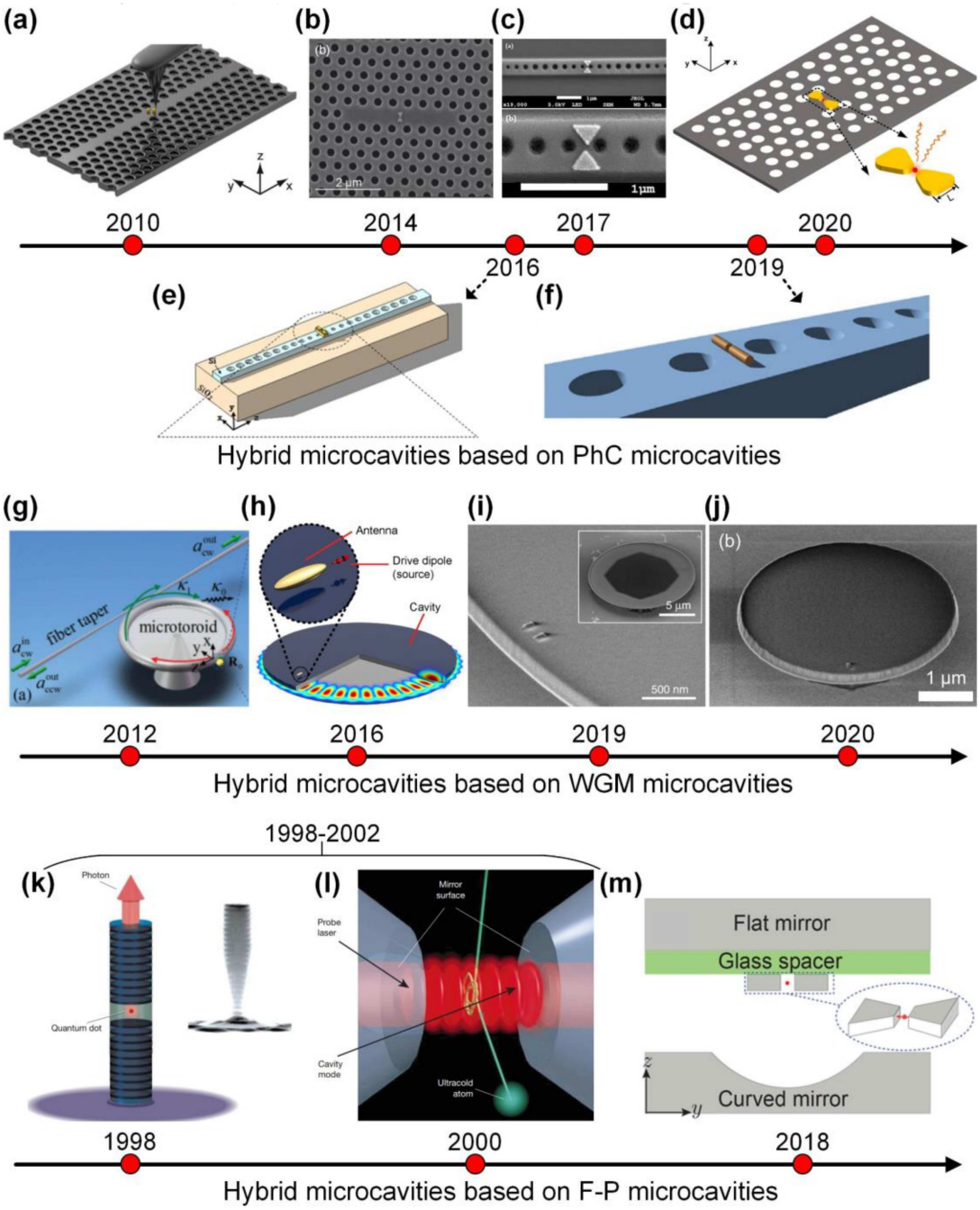

Fig. 1. (a) A plasmonic-photonic hybrid microcavity was realized in 2010.[67] (b) The 2D hybrid system was proposed in 2014.[70] (c) A hybrid microcavity was proposed in 2017.[69] (d) A hybrid photonic-plasmonic microcavity was proposed in 2020.[65] (e) A photonic-plasmonic microcavity with a 1D PhC dielectric cavity was realized in 2016.[71] (f) A hybrid microcavity consisting of a 1D PhC dielectric cavity and a metal dimer was realized in 2019.[72] (g) A hybrid structure based on WGM microcavity was proposed in 2012.[60] (h) A coupled cavity−antenna system was proposed in 2016.[62] (i) A hybrid structure of an antenna-dimer on a micro-disk was realized in 2019.[66] (j) A hybrid WGM microcavity was proposed in 2020.[73] (k) InAs quantum boxes were placed in the core of small-volume and high-finesse GaAs/AlAs pillar microresonators.[74] (l) Cesium atoms were captured in a magneto-optical trap (MOT) and dropped through a high-finesse optical cavity.[75] (m) A hybrid microcavity based on F-P microcavity was proposed in 2018.[68]

the advantage of the hybrid system in enhancing light–matter interaction furthermore. The study of hybrid microcavities based on WGM microcavities began in 2012,[60] and the development of the hybrid microcavities has gone through the process from theoretical design[62] to experimental realization.[66,73] In early 21st century, F-P microcavities have played key roles in Purcell enhancement, single-photon source[74] and strong coupling studies.[75] The research of hybrid microcavities based on F-P microcavities began in recent years.[63,68] The relevant works are focused on theoretical design of the hybrid system so as to greatly enhance light–matter interaction, since this type of hybrid microcavity is hard to be realized in experiment according to current techniques.

In this review, we firstly introduce photonic microcavities from physical concepts to applications and discuss the limitations in the pure systems. Then, three types of typical photonic-plasmonic hybrid microcavities are introduced to be the candidates in enhancing light–matter interaction, which are PhC microcavities combined with plasmonic nano-antenna, WGM microcavities combined with plasmonic nano-antenna, and Fabry–Perot (F-P) microcavities combined with plasmonic nano-antenna. In recent years, topological photonics provides a new platform to design robust optical devices. Thus, optical microcavities based on the topological state have become the hotspot. The cavity modes that exist in topological microcavities are robust. Here, the topological photonic crystal nano-cavities based on corner state are introduced from physical principles to applications. Besides, hybrid systems based on topological photonic microcavities have also been introduced. Different from the conventional hybrid systems, the combination of plasmonic nano-antennas and topological photonic crystals microcavities produced a robust platform in enhancing light–matter interaction. Finally, we summarize the advantages of photonic-plasmonic hybrid microcavities in enhancing light–matter interaction and prospect the development of hybrid systems in the future.

2. Photonic dielectric microcavity

2.1. Physics

Optical microcavities, which can confine light to regions of micron meter scale via resonant recirculation,[25] play key roles in enhancing light–matter interaction. The quality factor Q and the mode volume V are both important indexes in designing optical microcavities, and the figure of merit Q/V is introduced as a basic index to evaluate the property of optical microcavities.[26] There are three types of microcavities. The first type is PhC microcavity.[76] Since light in the bandgap frequency range is forbidden, the cavity modes are generated when introducing defects in the periodic structures. The second type is the WGM microcavity, the total reflection interface is formed between the high interior refractive index medium and the low external refractive index medium. Thus, a strong restriction of light is realized.[77] The third type is F-P microcavity, whose active area consists of two parallel planar mirrors with very high reflectivity, and the light is reflected in the two mirrors to form resonance. The first two types of optical microcavities are easy to integrate on-chip and provide potential platforms in enhancing light–matter interaction.

2.2. Application

PhC nano-cavities and WGM microcavities are beneficial for on-chip integration, which are widely applied in filters,[78–80] sensors,[81–88] nano-lasers,[89–92] and cavity QED.[93–97] Photonic crystal nano-cavities can confine light within a certain frequency range in bandgap and offer high spectral selectivity,[98,99] which are suitable candidates in realizing filters. A new type of optical channel drop filter (CDFs) based on a photoniccrystal ring resonator (PCRR) was designed in theory.[78] The drop efficiency was up to 100% at the wavelength of 1550 nm. A tunable all-optical microwave filter based on a photonic crystal L3 cavity was realized in the experiment and the ultra-high tuning efficiency was up to 101.45 GHz/mW.[79] Different from PhC nano-cavities, filters based on WGM microcavities are realized through coupling to the waveguide. The light of resonant wavelengths in the input waveguide can be coupled to the cavity and then transferred out by coupling to the output waveguide. Thus, the filtering effect is realized.[80] The performance of filters is determined by the coupling efficiency between WGM microcavities and waveguides.

PhC nano-cavities and WGM microcavities have high quality factor, so they have narrow linewidth and even very small drift of spectral lines can be easily observed. Therefore, they have great prospects in realizing sensors. For example, the ultracompact biochemical sensor based on 2D photonic crystal nano-cavity has been realized in the experiment.[81] A tiny change of refractive index Δn was readily apparent through observing the shift of the resonant wavelength, where $\Delta n = 0.002$. The sensitivity mentioned above is demonstrated to be better than that in a passive microcavity configuration. In recent years, refractive index sensor array based on photonic crystal microfiber cavity[82] and mid-infrared gas sensor based on high Q/V point-defect PhC nano-cavity have also been proposed,[83] which largely improve the development of on-chip sensors. WGM microcavities also play an important role in sensors. In the aspect of biological sensing, single virus and nanoparticle detection were realized through observing the mode shift,[84] mode splitting,[85] and mode broadening[86] of the WGM microcavities resonant spectrum.

In addition to the biological sensing mentioned above, WGM microcavities can also realize high-performance tem-

perature sensing[87] and mechanical sensing.[88] Besides, photonic microcavities with high quality factor Q have extensive applications in nano-lasers[89] and cavity QED.[11] For example, photonic crystal nano-cavities with Q factor greater than thousands can be used in low threshold nano-lasers.[90,91] When the Q factor reaches tens of thousands, the strong coupling can be realized, which is a typical manifestation of cavity QED.[94,95] Up to now, the optimization of Q factor continues, and the value of the Q factor can reach millions[100,101] or even billions by the approach of deep learning.[102] However, the mode volume V of the photonic dielectric microcavities is always near a cubic of wavelength and hard to decrease due to the laws of diffraction, which limits the enhancement of the figure of merit Q/V.[34,43]

3. Photonic-plasmonic hybrid microcavities

3.1. Surface plasmon resonances

Surface plasmon resonance (SPR) is a surface electromagnetic wave formed by the coupling of free electrons and photons on the surface region, which is often found on the surface of planar metals and dielectric materials.[48] The coresonant oscillations generated by the mutual excitation between free electrons and electromagnetic fields give metals unique optical properties. However, due to the inherent ohmic loss of the metallic structure and the radiation loss to the substrate, the energy loss in the transmission of surface plasmon resonances is significant, which has a major impact on the performance and signal transmission of nanophotonic devices.[103]

Localized surface plasmon resonance is a physical phenomenon that occurs in subwavelength metal particles.[49,50] The mode volume V of the metal particles is far below the diffraction limit due to localized surface plasmon resonances.[54] Advances in both synthetic and lithographic fabrication techniques allow researchers to vary the shape, size, and material of the nanoparticles that support the localized surface plasmon resonances, which provides various platforms to realize ultra-small mode volume.[50] However, the quality factor of the metal particles is generally below 50 due to serious metal loss.[56]

3.2. Applications of photonic-plasmonic hybrid microcavities

Due to the localized surface plasmon resonances, plasmonic cavities have great advantages in confining light into very small space and realizing ultra-small mode volume V, which makes them widely be applied in quantum optics[11,13,15,104–107] and nonlinear optics,[108–111] such as Purcell enhancement in weak coupling,[51,52,112] Rabi splitting in strong coupling[54,113–115] and single nonlinear optical response enhancement.[109] However, the development of the above applications is hard to have a breakthrough due to the low quality factor Q, which is caused by the serious metal loss of the plasmonic cavities.[56–59] Thus, hybrid microcavities, which consist of high quality factor Q photonic microcavities and small mode volume V plasmonic cavities (plasmonic nano-antennas), have been proposed to largely improve the light–matter interaction.[61–68] In this section, three typical types of hybrid systems are introduced and illustrated respectively, which contain the PhC nano-cavities combined with plasmonic nano-antenna,[65,67,69–72] WGM microcavities combined with plasmonic nano-antenna[60,62,66,73] and F-P microcavities combined with plasmonic nano-antenna.[63,68,116] Taking advantages of both high quality factor Q of photonic microcavities and ultra-small mode volume V of plasmonic resonators, the hybrid microcavities provide a promising platform for the study of biosensing,[2–4] optical trapping,[8,9] cavity quantum electrodynamics (QED),[11,12] on-chip nanolasers[17–19] and surface-enhanced Raman scattering (SERS).[23,24]

In 2016, Conteduca *et al.* proposed a hybrid microcavity based on a 1D photonic crystal (PhC) dielectric cavity and a plasmonic nano-antenna.[71] The schematic diagram of the proposed structure is shown in Fig. 2(a). Large electromagnetic energy enhancement was realized in the gap of the plasmonic nano-antennas when the resonant spectra of the dielectric cavity and plasmonic nano-antennas have a large overlap [see Fig. 2(b)]. Under efficient coupling between the dielectric cavity mode and the localized surface plasmon resonances mode, an ultra-high Q/V ratio of $10^6(\lambda/n)^{-3}$ and a remarkable resonance transmission ($T = 47\%$) have been achieved simultaneously in the hybrid structure, as shown in Fig. 2(c), which indicates that the hybrid system is a suitable candidate in realizing biosensing. In 2017, the hybrid microcavity in Ref. [71] was successfully fabricated in the experiment. The SEM image of the hybrid structure is shown in Fig. 2(d). When the resonant wavelength of the plasmonic bowtie nan-antennas matched that of the 1D PhC nano-cavity, large energy confinement was generated in the gap between the two gold triangles [see Fig. 2(e)]. The compromise between strong light confinement and low metal loss in plasmonic bowtie nano-antennas was reached with an appropriate size of the gap. The high figure of merit Q/V of $10^6(\lambda/n)^{-3}$ and a transmission of 20% of the hybrid microcavity were obtained [see Fig. 2(e)]. Based on the high figure of merit and transmission, the hybrid structure was demonstrated to be a high efficiency nano-tweezer for optical trapping. A stable trapping condition can be achieved for a single 200 nm Au bead for several minutes (trap $<$ 5 min) and with very low optical power (Pin $= 190$ μW) [see Fig. 2(f)].[69] In addition to the application in biosensing and optical trapping, the 1D hybrid system has also been applied in quantum optics.

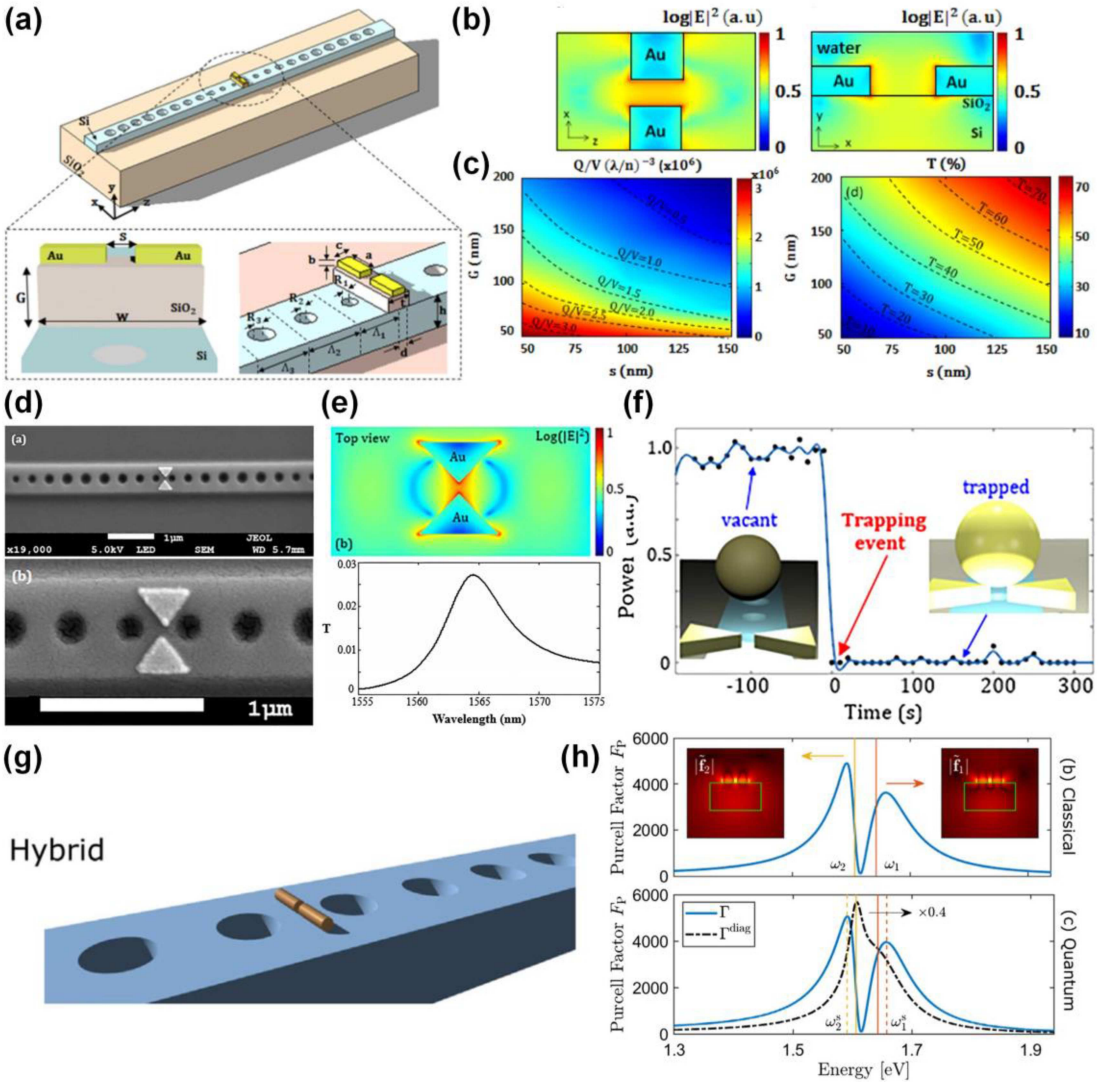

Fig. 2. (a) The schematic diagram of the photonic-plasmonic cavity with a 1D PhC dielectric cavity.[71] (b) The electric field distribution at resonance of the photonic-plasmonic cavity.[71] (c) The figure of merit Q/V and resonance transmission T as a function of the gap G and the slot widths.[71] (d) The scanning electron micrograph (SEM) of the hybrid cavity.[69] (e) The electric field distribution of photonic-plasmonic cavity and transmission spectrum of the hybrid cavity when trapping a 200 nm Au bead.[69] (f) Power versus time at the output of the hybrid cavity.[69] (g) The schematic diagram of hybrid nano-cavity consisting of a 1D PhC dielectric cavity and a metal dimer.[72] (h) Semiclassical Purcell factor and QNM-JC Purcell factor as a function of the energy, with quasinormal modes (QNMs) profiles in the inset.[72]

In 2019, Franke *et al.* utilized the hybrid microcavity to illustrate the practical application of the second quantization scheme based on quasinormal mode (QNMs). As is shown in Fig. 2(g), the hybrid microcavity consists of a gold nanorod dimer and a 1D PhC nano-cavity,[72] which supports two overlapping quasinormal modes (QNMs) with two frequencies ω_1 and ω_2, as is shown in the first picture of Fig. 2(h), and the two corresponding QNMs profiles are shown in the inset. The Purcell factor versus energy was calculated with a semiclassical approach and the QNM-JC model respectively, as is shown in Fig. 2(h). Due to different phase terms of overlapping QNMs, Fano-type resonance (blue line) appeared in both conditions. However, the Purcell factor in QNM-JC model contains the diagonal contribution $\Gamma^{\rm diag}$, which is one component of the full emission rate Γ, where $\Gamma = \Gamma^{\rm diag} + \Gamma^{\rm n\,diag}$. Thus, the two resonant frequencies of the QNMs-JC Purcell factor have been shifted compared with that of the semiclassical Purcell factor. The 1D hybrid system provides an ideal platform for studying the quantization scheme based on QNMs.

The optimization of the figure of merit Q/V in 1D hybrid systems is limited by dimension, which makes them hard to realize strong interaction between light and matter. The 2D hybrid systems have the potential to be the better candidates by contrast. In 2010, Barth *et al.* firstly proposed a hybrid cavity system that consists of metal nanoparticles and a planar double-heterostructure PhC cavity. The hybrid structure was successfully fabricated through a nano assembly method, which combined the modified dippen technique with atomic force microscope (AFM) manipulation. The individual metal nanoparticles can be deterministically placed on the dielectric PhC cavity [see Fig. 3(a)]. A hot spot is created in the gap because the metal constituents lead to strongly localized

fields [see Fig. 3(b)]. The interaction between the plasmonic nanoantenna and the cavity mode is manifested in the pronounced Fano-like line shape (red curve in dashed frame), which is observed in the spectrum in Fig. 3(c).[67] The experimental realization of the hybrid structure gives a new insight in enhancing light–matter interaction. In 2014, Zhang *et al.* proposed a nano-laser based on a hybrid photonic-plasmonic nano-cavity. As is shown in Fig. 3(d), the hybrid system consists of a 2D dielectric photonic crystal cavity and a plasmonic bowtie nano-antennas.[70] The hybrid microcavities with different locations of plasmonic bowtie antennas were successfully fabricated through a novel method based on multi-step electron-beam lithography, which can accurately control the position of the antennas. The SEM image of the hybrid structures is shown in Fig. 3(e). The mode volume of the hybrid microcavity was far below the diffraction limit, but the quality factor of the hybrid microcavity was relatively low due to the serious metal loss. Thus, the laser threshold was increased with the presence of the plasmonic bowtie nano-antennas [see Fig. 3(f)]. The variation in the laser peak intensity with effective incident pump power was obtained [see Fig. 3(f)]. The optical properties of the basic hybrid structures were measured by micro-photoluminescence spectroscopy at room temperature.

Besides the applications in nano-lasers, the hybrid systems have great potential in cavity quantum electrodynamics (QED),[117–124] such as Purcell enhancement in weak coupling region and Rabi splitting in strong coupling region.[51,52,113–115] Basic concepts of cavity QED are explained as follows. The cavity QED is focused on studying the interaction between a quantized cavity mode and atoms. Since the optical mode in the cavity is discrete and concentrated, some interesting physical phenomenon will happen when the atoms interact with the cavity mode through absorbing and emitting photons. Here, we introduce the most basic model of cavity QED: Jaynes–Cummings (J-C) model, which describes the interaction of a single mode and a two-level atom (dipole).[125] We further introduce the criterion for determining strong coupling and weak coupling.

The Hamilton of the J-C model is expressed as below:

$$H_{\mathrm{JC}} = \omega_{\mathrm{c}} a^{\dagger} a + \omega_{\mathrm{e}} \sigma_{+} \sigma_{-} + g\left(a^{\dagger} \sigma_{-} + a \sigma_{+}\right), \tag{1}$$

where $a^{\dagger}$ and a are creation and annihilation operators of cavity mode, σ_{+} and σ_{-} are Pauli operators, ω_{c} and ω_{e} are resonant frequencies of cavity and dipole. g represents the coupling strength between atoms and cavity mode, and the expression is $g = \mu\sqrt{\frac{\omega_{\mathrm{c}}}{2\hbar\varepsilon V}}$, where μ is the dipole moment of the atoms, ε is the dielectric constant and V is the mode volume of the cavity.[60] The value of g/κ is the criterion to evaluate whether the system is in the weak coupling or strong coupling regime. κ is the decay rate of the cavity.

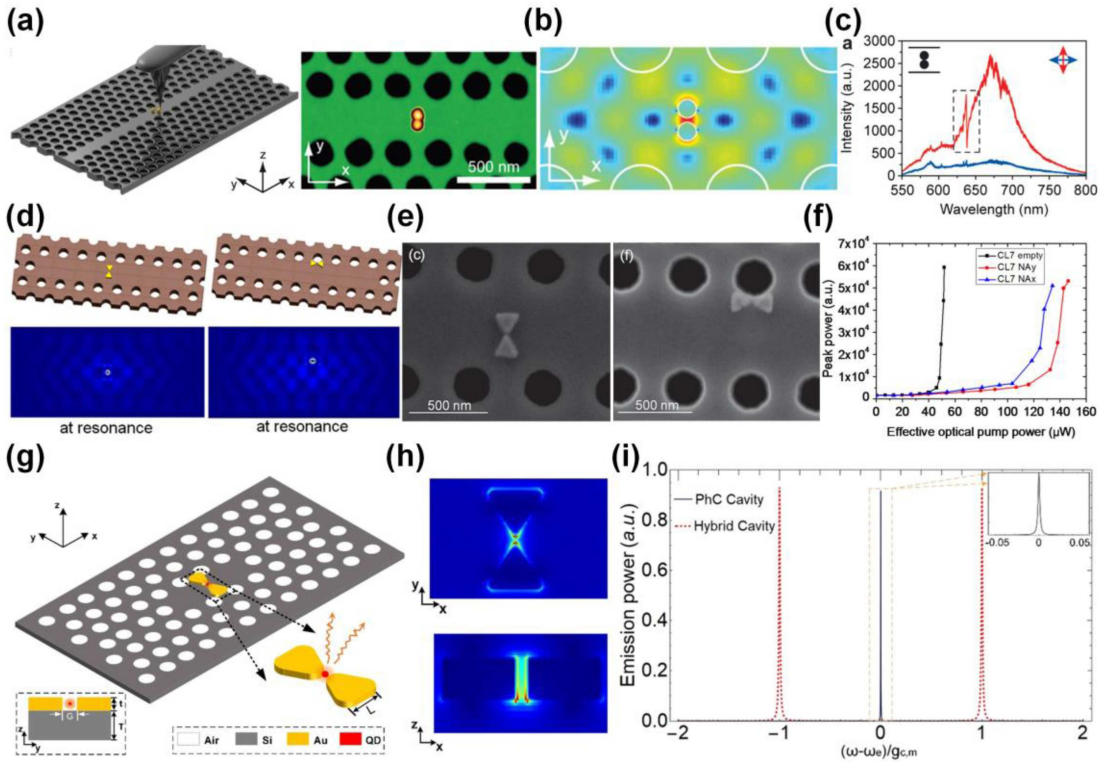

Fig. 3. (a) The employed AFM manipulation technique and the schematic diagram of the plasmonic-photonic hybrid cavity.[67] (b) Calculated electric field intensity distribution $|E|^2$ of the hybrid nano-cavity.[67] (c) Fluorescence spectrum from the configuration shown in Fig. 2(a).[67] (d) Two designs of hybrid nano-cavities and their corresponding electric field distributions.[70] (e) The SEM of the hybrid nanostructures.[70] (f) Variation of the laser peak intensity versus the effective incident optical pump power of three kinds of the proposed structures.[70] (g) Sketch of hybrid photonic-plasmonic nano-cavity.[65] (h) The electric field distributions of the hybrid nano-cavity.[65] (i) The radiation power of the quantum emitters in bare photonic crystal nano-cavity and hybrid nano-cavity versus the detuning $(\omega-\omega_{\mathrm{e}})$.[65]

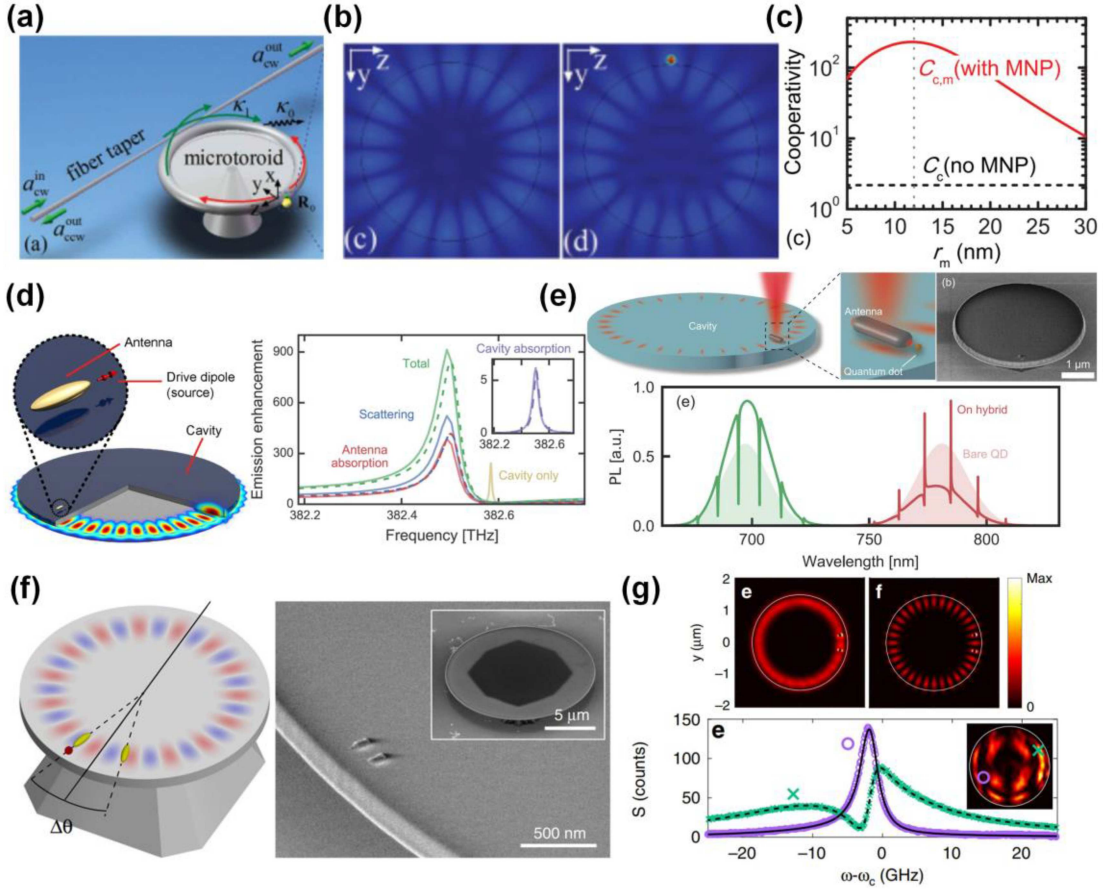

Fig. 4. (a) Sketch of hybrid structure based on WGM microcavity.[60] (b) Top view of the electric field profile without and with metal nanoparticles.[60] (c) Cooperativity without and with the presence of the MNP versus the radius of the MNP.[60] (d) Left: the schematic diagram of a hybrid system driven by a dipole source. Right: emission enhancements in the hybrid system.[62] (e) Up: sketch and SEM image of the hybrid WGM microcavity. Down: calculated quantum dot emission spectra at resonance (green line) and off-resonance (red line) of the antenna resonance.[73] (f) Sketch and SEM image of the hybrid structure of an antenna-dimer on a microdisk.[66] (g) Up: the simulated cycle-averaged field intensity $|E|^2$ on the top interface of the hybrid structure with different antenna separation. Down: the angular radiation pattern (inset) and corresponding scattering spectra at chosen (k_x, k_y).[66]

When $g/\kappa < 1$, the system is in a weak coupling regime. A typical physical phenomenon in the weak coupling regime is the Purcell effect, i.e., the spontaneous emission rate of atoms will be enhanced when it couples to the cavity mode.[126] Purcell factor F is introduced to represent the ratio of the spontaneous emission rate of atoms in a vacuum and a cavity, and the expression is $F=\frac{3}{4\pi^2}\left(\frac{\lambda}{n}\right)^3\frac{Q}{V}$.[126] When $g/\kappa > 1$, the system is transformed into a strong coupling regime. A typical physical phenomenon in the strong coupling regime is Rabi splitting, i.e., the emission power spectrum of atoms will split into two peaks.[11] Recently, Zhang *et al.* proposed a hybrid photonic-plasmonic nano-cavity with the ultra-high figure of merit Q/V, which can realize strong coupling and the Rabi splitting appeared in the emission power spectrum [see Fig. 3(i)]. The sketch and electric field distribution of the hybrid structure are shown in Figs. 3(g) and 3(h).[65] The hybrid microcavity with high figure of merit provides a new avenue in realizing strong coupling and has potential applications in quantum information processing.

Except for the hybrid systems based on PhC cavities, some groups work on the hybrid systems based on WGM microcavities. As early as 2012, Xiao *et al.* proposed a photonic-plasmonic hybrid microcavity which consists of a metal nanoparticle (MNP) and a WGM microcavity [see Fig. 4(a)]. The mode volume of the hybrid system is decreased since the MNP offers a highly enhanced local field [see Fig. 4(b)]. Interestingly, for the hybrid system, the high quality factor property of WGMs can be maintained in the presence of the MNP.[60] Thus, the single-atom cooperativity is enhanced by more than two orders of magnitude compared to that in a bare WGM microcavity [see Fig. 4(c)], which provides a potential platform in quantum optics. In 2016, Doeleman *et al.* proposed a hybrid microcavity as a versatile platform for emission enhancement.[62] The hybrid system consists of a WGM microcavity and a dipolar antenna [Fig. 4(d)]. The emission enhancement of the hybrid system from the oscillator model (dashed line) and finite element simulation (solid line) is calculated in Fig. 4(d). The emission enhancement in the oscillator model is expressed as follows:

$$\eta_{\text{total}} = 1 + \frac{6\pi\varepsilon_0 c^3}{\omega^3 n}\,\text{Im}(\alpha_{\text{H}} G_{\text{bg}}^2 + 2G_{\text{bg}}\alpha_{\text{H}}\chi_{\text{hom}} + \chi_{\text{H}}), \quad (2)$$

where α_H, χ_H, and χ_{hom} are the hybridized antenna polarizability, cavity response function and bare cavity response, and G_{bg} is the Green's function of the background environment. As is shown in Fig. 4(d), the results of emission enhancement calculated with finite element simulation (solid line) are merely identical to that calculated with oscillator model (dashed line), which demonstrates the accuracy of the numerical simulation. The total enhancement (green) in the hybrid system resulted from the scattering into the free space (blue), antenna absorption (red), and cavity absorption (purple), which was much larger than that in the bare cavity (yellow). The theoretical design in Ref. [62] was successfully realized in the experiment by Doeleman *et al.* in 2020. The SEM image of the hybrid structure is shown in Fig. 4(e). The emission enhancements of a single quantum dot in such a hybrid system were observed through the photoluminescence (PL) spectra. As is shown in Fig. 4(e), the shaded areas indicate bare QD spectra, the green line and red line indicate the quantum dot emission spectra at resonance and red detuned from the antenna resonance, respectively. The emission enhancement in the hybrid system profits from both plasmonic confinement and high quality factor of the WGM microcavity.[73] The work demonstrates the potential of the hybrid system for enhancing light–matter interaction. The hybrid systems mentioned above are both based on one dipole antenna. The interaction between two dipole antennas and WGM microcavity has been reported recently. Gognee *et al.* proposed a high Q hybrid plasmonic-photonic microcavity, consisting of a dielectric microdisk and a pair of plasmon nano-antennas, to be used to realize unidirectional light sources.[66] The sketch and the SEM image of the hybrid structure are shown in Fig. 4(f). Large local density of state (LDOS) enhancement is achieved and it exceeds those given by a single nano-antenna. As is shown in the first picture of Fig. 4(g), the cycle-averaged field intensity $|E|^2$ is calculated and it is homogenous with antenna separation of 0.94 cavity period (left). In contrast, the cycle-averaged field intensity $|E|^2$ exhibits a standing wave pattern with the antenna separation of 1 cavity period (right). It indicates that the distribution of cycle-averaged field intensity is determined by the antenna separation. The unidirectional property of the hybrid microcavity occurred at the antenna separation of 0.94 or 1 and the radiation pattern of the hybrid microcavity is shown in the inset of Fig. 4(g), which is consistent with the theoretical prediction. The scattering spectra of the wave vectors marked with a green cross and purple circle are shown in Fig. 4(g), the coherent superposition of QNMs is directly revealed by the Fano lineshapes (purple line) in the scattering spectra, which provides new insight for single nanoparticle or molecular detection.

In recent years, hybrid systems based on F-P microcavities are indicated to be suitable candidates in promoting the development of quantum devices.[63,68] In 2017, Peng *et al.* studied the hybrid system which consists of metallic nanoparticles (MNPs) and an optical microcavity. They proposed a universal theoretical model to reveal the role of the dielectric microcavity in a hybrid system, so the optical microcavity used here is not limited to a FP-type microcavity. The schematic diagram of the hybrid structure and the interaction in the system are shown in Fig. 5(a). The quantum emitter is firstly assembled onto the surface of MNP, and the composite is placed in the optical microcavity.[63] The significantly enhanced coherent radiation and the reduced incoherent dissipation are revealed through an analytical quantum model based on the hybrid system. Importantly, the strong coupling can be realized in the cavity engineered MNP-emitter system, i.e., the vacuum Rabi oscillation and splitting are observed in the emission spectrum of the quantum emitter [see Fig. 5(b)]. The hybrid microcavity plays an important role in promoting the development of quantum optics. In 2018, Gurlek *et al.* studied a similar system with the last work but with different theoretical methods, where they combined numerical simulation with the quasinormal mode approximation. The sketch of the hybrid microcavity is shown in Fig. 5(c), which consists of a plasmonic bowtie nano-antenna and an F-P microcavity.[68] Due to the high figure of merit of the proposed structure, Rabi splitting occurred in the emission spectrum of the quantum emitter [see Fig. 5(c)]. Besides the applications in cavity QED, the hybrid system consists of F-P microcavity and plasmonic bowtie nano-antennas plays a key role in surface-enhanced Raman scattering (SERS). Liu *et al.* proposed a hybrid microcavity that consists of gold nanorods (AuNRs) and a resonant dielectric photonic crystal (PC) slab. The schematic diagram of the hybrid structure is shown in Fig. 5(d). The PC slab possesses two types of cavity resonances: a broadband FP cavity and a narrowband PC-guided resonance (PCGR). Both kinds of cavity modes can be matched with the AuNR resonance.[116] The large enhancement of local field intensity is realized through observing the SERS. The coupling between PCGR mode and localized plasmon mode offers at least 1 order of magnitude greater amplification of AuNRs' local field intensity compared to that offered by coupling to the F-P mode. The proposed hybrid microcavity brings new opportunities for enhancing light–matter interactions and benefits to the areas such as nonlinear optics and surface-enhanced Raman spectroscopy.

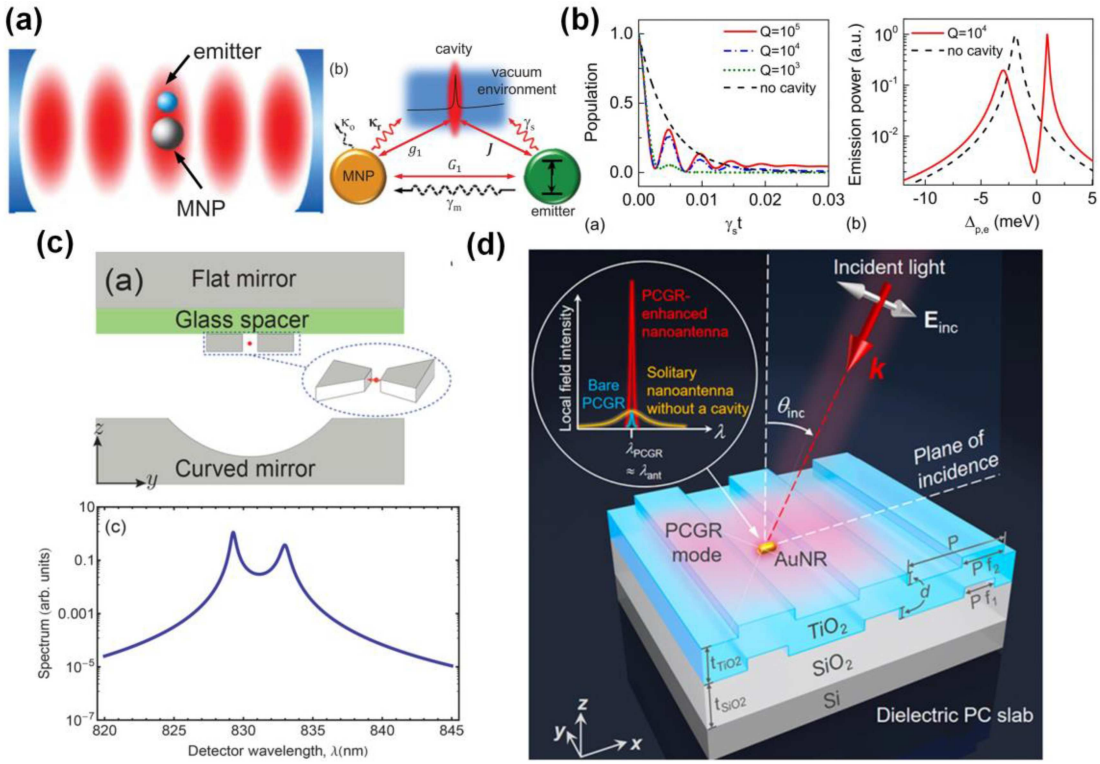

Fig. 5. (a) The schematic diagram of a quantum emitter coupled to an MNP in a microcavity-engineered environment.[63] (b) Left: temporal evolution of the population $\langle \hat{\sigma}_+(t)\,\hat{\sigma}_-(t)\rangle$ on the emitter for a cavity with different quality factor Q, and without the cavity. Right: radiation power of the emitter versus pump-emitter detuning.[63] (c) Up: a sketch of the hybrid cavity based on F-P microcavity. Down: fluorescence spectrum of an emitter that interacts with the detuned hybrid mode.[68] (d) Local field enhancement realization of the synergistic hybrid microcavity.[116]

4. Topological photonic-plasmonic crystal hybrid microcavities

4.1. Topological photonic crystal microcavity

Topological photonics provides robust platforms in designing photonic devices. Novel photonic crystal (PhC) microcavities based on the topological state are booming in recent years. Topological microcavities have advantages in realizing nano-lasers and light trapping[127–133] because the cavity modes of topological photonic crystal microcavity are robust and immune to disorders. In 2018, Ota *et al.* designed a topological PhC nano-cavity based on 1D Su–Schrieffer–Heeger (SSH) model. Topological property in the cavity is characterized by the Zak phase, which is defined as an integral of the Berry connection over the first Brillouin zone

$$Z_n = \oint \mathrm{i}\langle u_n(k) \mid \frac{\mathrm{d}}{\mathrm{d}k} \mid u_n(k)\rangle \mathrm{d}k, \tag{3}$$

where Z_n is the Zak phase and $\mid u_n(k)\rangle$ is the periodic Bloch function that belongs to the n-th band.[127] By tuning the lengths of the rectangular air holes and the distance between them, the Zak phase can be changed [see Fig. 6(a)]. When putting the two materials with different topological indexes together, the topological phase transition takes place at the interface. Thus, the topological protected 0D corner states emerge at the interface. The 1D topological photonic crystal nanocavity is formed based on the corner state, and the quality factor Q is up to 59700 in theory. A high-β laser based on high quality factor is realized successfully in the experiment, where β is the spontaneous emission coupling factor [see Fig. 6(b)]. The designed structure was fabricated on a GaAs slab, which contains 5 layers of InAs QDs.

In 2019, Han *et al.* designed a nanolaser based on a topological PhC L3 nano-cavity dimer array.[128] In this report, the topological invariant was described as winding number

$$W = \frac{\mathrm{i}}{\pi}\oint \langle u(k) \mid \frac{\mathrm{d}}{\mathrm{d}k} \mid u(k)\rangle \mathrm{d}k, \tag{4}$$

where the path of integral covers the first Brillouin zone and $\mid u_n(k)\rangle$ is the periodic Bloch function. The Hamiltonian of the system can be written as follows:

$$H = \begin{pmatrix} \omega_0 & C_A + C_B \mathrm{e}^{-\mathrm{i}ka_0} \\ C_A + C_B \mathrm{e}^{\mathrm{i}ka_0} & \omega_0 \end{pmatrix}, \tag{5}$$

where ω is the resonant frequency of the L3 cavity, C_A and C_B are the coupling strengthes between cavities, which can be tuned by the distance between the cavities [see Fig. 6(c)]. The topological non-trivial phase was realized by tuning the distance between the L3 cavities. The direct evidence for lasing at topological edge state was obtained by near-field scanning optical microscope (NSOM) [see Fig. 6(d)]. The robustness of the proposed structure has also been verified.[128] However, the laser mode is in a 0D defect state for the 1D structure, which cannot provide protected transport.[130] Higher-

order topological insulators (HOTIs) have been proposed to describe topological insulators (TIs) that have lower dimensional gapless edge states. For example, a second-order 2D TI may have gapped 1D edge states but gapless 0D corner states. Many people engage in the exploration of higher-order topological photonic crystals.[134,135] In 2018, Xie *et al.* realized a 2D photonic topological insulator (PTI) which is the 2D photonic generalization of the SSH model.[134] In this PTI, there are four identical dielectric rods in each unit cell which form isotropic ($l_x = l_y$) or anisotropic ($l_x \neq l_y$) PhCs [see Fig. 7(a)]. Topological edge and corner states can appear in the first photonic bandgap (PBG) by tuning the distance between the four rods [see Fig. 7(b)]. The topological corner charge is determined by the edge polarization as $Q_c = p_x^{v_y} + p_y^{v_x} = 4P_xP_y$. The whole phase diagram including isotropic and anisotropic PhCs is classified into four parts which are depicted in Fig. 7(c). The characteristic of the topological phase can be potentially used to design different optical topological switches for the photonic integrated chip. In 2019, based on the generalized 2D SSH model, Chen *et al.* directly observed the corner state by using near-field scanning measurements [see Fig. 7(d)].[135] In this work, the protected topological corner state is related to the 2D Zak phase $Z^{\mathrm{Zak}} = (Z_x, Z_y)$, which is defined as

$$Z_i = \iint \mathrm{Tr}[\hat{A}_i(\boldsymbol{k})]\,\mathrm{d}k_x\mathrm{d}k_y, \tag{6}$$

$$(\hat{A}_i)_{mn}(\boldsymbol{k}) = \langle u_m(\boldsymbol{k}) \mid \partial k_i \mid u_n(\boldsymbol{k})\rangle, \tag{7}$$

where $i = x$ or y. $\hat{A}_i(\boldsymbol{k})$ is the Berry connection and the range of integration covers the first Brillouin zone. The topological and trivial phases are (π, π) and (0, 0), respectively. The topological phase of the structure is changed when tuning the distance between dielectric cylinders in a unit cell. The quantized edge dipole polarization along the x-axis and y-axis can induce the 0D corner state in the band gap when combing the two kinds of PhCs with different topological phases. Since the corner state is robust and immune to disorders, it is a good platform to realize 2D topological PhC cavities. In 2020, Xie *et al.* experimentally realized a 2D topological PhC nano-cavity based on corner state and the high quality factor Q of 10^4 was obtained by moving the topological PhC away from the corner by (g, g). Purcell enhancement of single quantum dot (QD) was demonstrated in the proposed structure [see Fig. 7(e)],[129] which provides a robust platform to investigate cavity QED and has potential applications in quantum information processing.

Besides, the topological PhC cavities are considered as good candidates to realize low-threshold nanolasers. In 2020, Zhang *et al.* designed and demonstrated a small footprint, low threshold and high energy efficiency topological nanolaser based on second-order corner state [see Fig. 7(f)]. They experimentally observed the lasing behavior of the corner state with the QDs as the gain medium through pump-power dependence of the corner state emission. As is shown in Fig. 7(g),

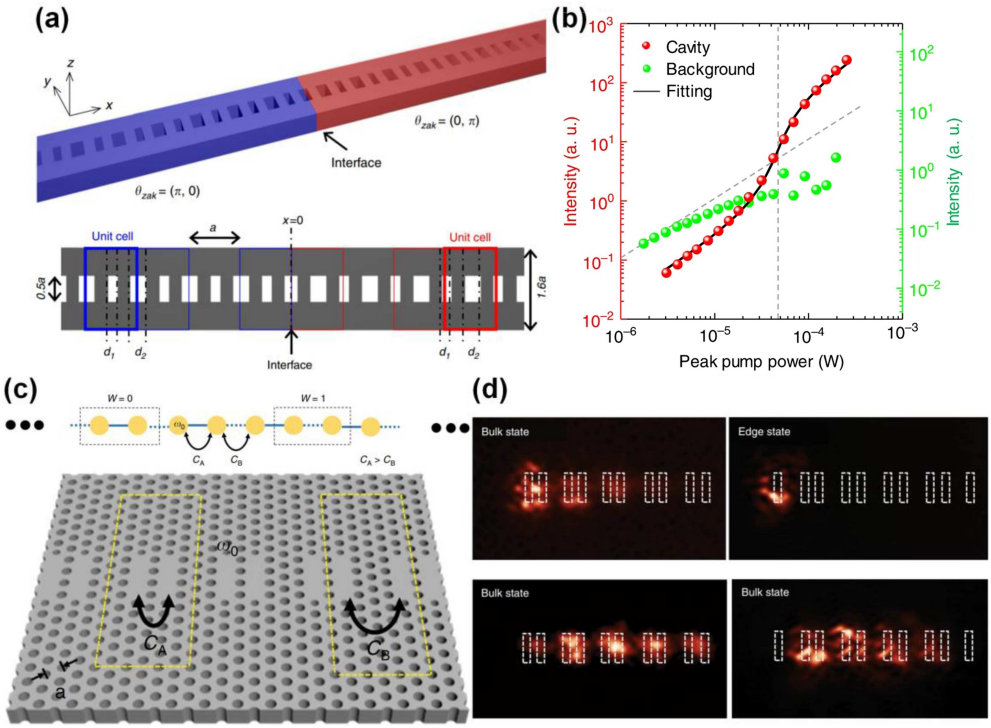

Fig. 6. (a) Up: schematic diagram of the 1D topological PhC nano-cavity. Down: illustration of design methods, i.e., the interface is formed by joining two PhCs together, and the two PhCs are different in the way that the unit cells are defined.[127] (b) Logarithmic plots of the light-in-light-out curve (red) and the evolution of the intensities of the background emission (light green).[127] (c) Schematic diagram of 1D SSH implemented in a 2D hexagonal PhC platform. It was composed of a linear chain of PhC L3 cavities with staggered coupling strengths C_A and C_B ($C_A > C_B$).[128] (d) NSOM images were recorded for structure $W = 0$ and $W = 1$ at the corresponding peak emission wavelengths.[128]

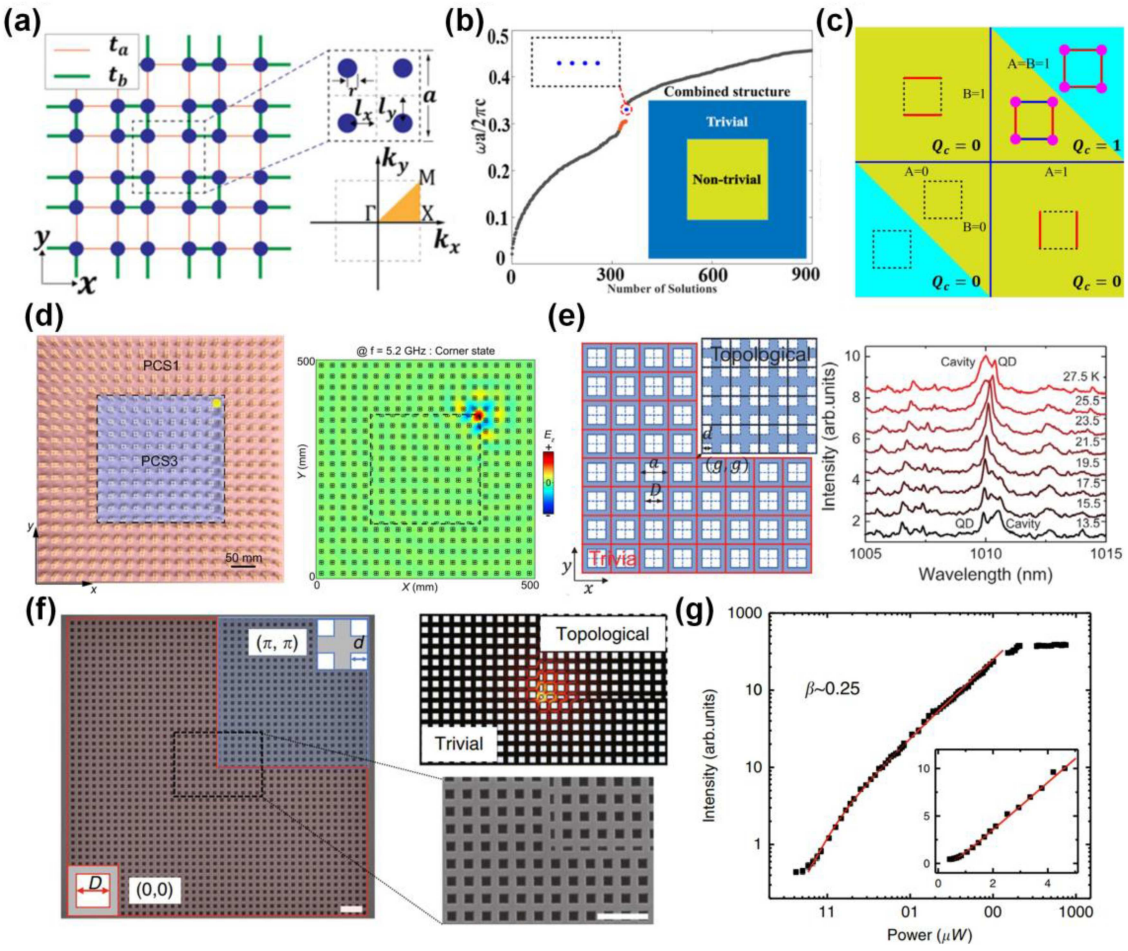

Fig. 7. (a) Schematic diagram of 2D photonic SSH model.[134] (b) Photonic eigenmodes of a combined structure where the PC is inside a box and the PTI is outside the box. There are four degenerate states localized at the four corners in the bandgap.[134] (c) Classification of all kinds of the generalized 2D photonic SSH model with different configurations in the x and y directions.[134] (d) Left: the sample for measuring corner states. Right: measured E_z field of the corner state at 5.2 GHz.[135] (e) Left: schematic diagram of 2D topological PhC nano-cavity. Right: PL spectra collected when the QDs are tuned across the corner state by temperature.[129] (f) Scanning electron microscopy image of a fabricated 2D topological PhC nano-cavity and electric field profile of the topological corner state.[131] (g) Pump-power dependence of the corner state for the cavity.[131]

a mild "s" shape appears in the light-in-light-out (L-L) plot, which indicates a lasing oscillation with high β and the value of β is approximately 0.25.[131] Besides, Chen *et al.* put forward a new approach in designing higher-order PTI, i.e., topology optimization approach.[136] The overlapped bandgap width between the nontrivial and trivial PhC achieves 29.3% by topology optimization approach, which is more than twice compared with the original higher-order PTI.[137,138] The study of the combination of topology and topology optimization approach will become more attractive since it provides an efficient way to design our higher-order devices to cater to our needs. Moreover, it can break the restrictions of traditional methods and predict novel higher-order PTI. These methods provide new avenues for the realization of higher-order PTI.

4.2. Topological hybrid nano-cavity

Novel optical cavities based on topological photonic states attract much attention due to their advantage of robustness.[127–131] However, the figure of merit Q/V is still limited, since the mode volume V of the dielectric topological cavities is hard to further decrease due to the light diffraction limit.[34–36] As a result, the figure of merit Q/V of the above topological cavities is not high, which extremely limits the strength of light–matter interaction and restricts the applications of topological photonic cavities in certain areas, such as Purcell enhancement,[51,52] strong coupling,[14,15] nonlinear quantum optics,[105,106] etc. Recently, Qian *et al.* propose a well-designed topological photonic hybrid structure containing a plasmon nano-antenna and 1D topological PhC nano-cavity, the sketch of the hybrid structure is shown in Fig. 8(a). The localized surface plasmon resonances almost do not have any influence on the edge state but the edge state greatly changes the local field distribution of the surface plasmon resonances [see Fig. 8(b)].[139] Based on this mechanism, an obvious absorption reduction in the spontaneous emission spectra occurs due to the near-field deformation around the antenna induced by the edge state. Moreover, the large Purcell factor reaches more than 10^4% due to the plasmon antenna with ultra-small mode volume [see Fig. 8(c)].[139]

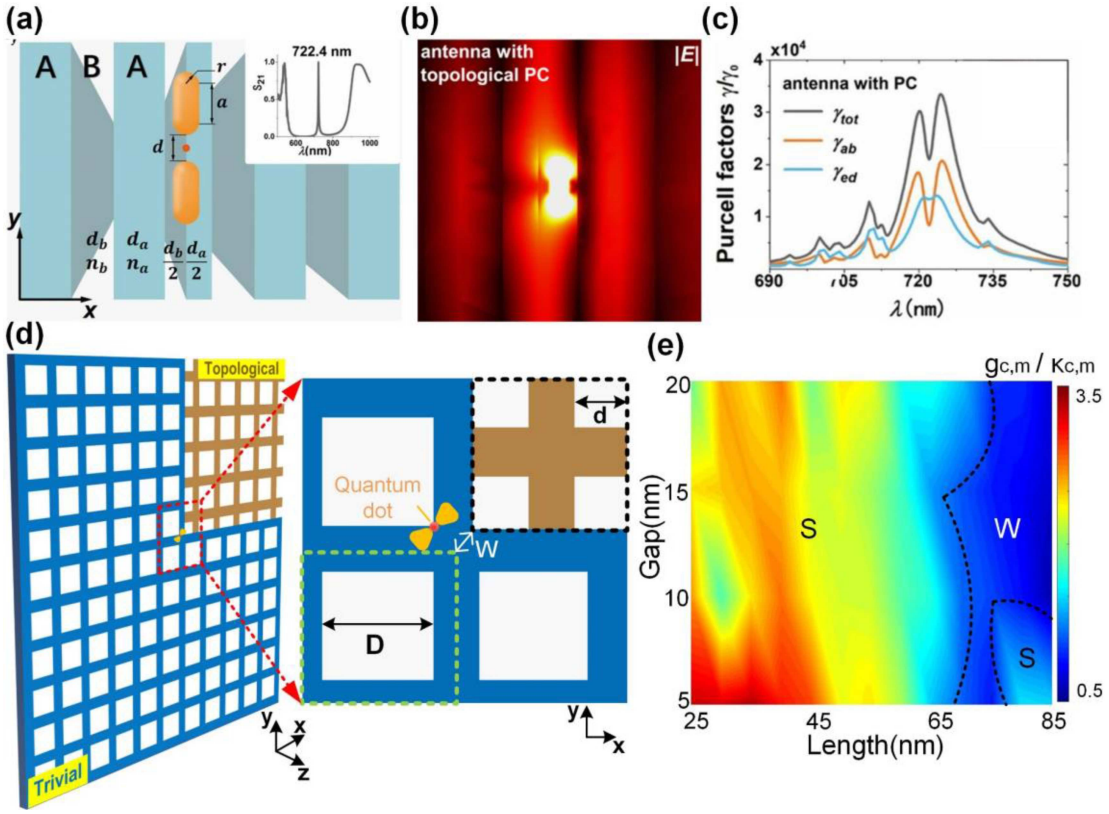

Fig. 8. (a) Schematic diagram of a topological hybrid structure composed of a 1D topological PC, a sliver nano-antenna, and a quantum emitter.[139] (b) The electric field $|E|$ of the hybrid structure.[139] (c) Purcell factor with a topological PC as a function of λ.[139] (d) Schematic diagram of a 2D topological photonic-plasmonic hybrid nanocavity. A quantum dot (red spot) is placed in the gap of the Au plasmonic bowtie nano-antenna.[140] (e) Color map of coupling phase transition. Strong coupling area is marked as "S" ($g_{c,m}/\kappa_{c,m} > 1$), and the weak coupling area is marked as "W" ($g_{c,m}/\kappa_{c,m} < 1$).[140]

Very recently, a two-dimensional topological hybrid nanocavity has been designed, which has an ultra-high figure of merit. The schematic diagram of the proposed structure is shown in Fig. 8(d), it consists of a topological PhC nanocavity and a gold (Au) bowtie nano-antenna. The highest figure of merit Q/V of the topological hybrid nanocavity is obtained when the length and gap of the Au plasmonic bowtie nano-antenna are 50 nm and 5 nm, respectively.[140] Based on the ultra-high figure of merit topological hybrid structure, the interaction between a single quantum dot and topological hybrid cavity mode can be tuned. As is shown in Fig. 8(d), a quantum dot (red dot) is placed in the gap of the Au bowtie nano-antenna. The strong coupling and weak coupling can be easily switched by adjusting the length and gap of the Au bowtie nano-antenna, where "S" and "W" represent the strong coupling area and weak coupling area, respectively and the black dotted line represents the value of $g_{c,m}/\kappa_{c,m}$ equal to 1.[140] This work provides an efficient method to manipulate coupling phase transition and will play a key role in quantum information and topological lasers.

However, the reports of the topological hybrid systems are very limited. The main tasks in future studies are to fabricate the sample of the topological hybrid structures and experimentally demonstrate the robust ultra-high figure of merit Q/V in the topological hybrid systems. Once these problems have been addressed, topological hybrid plasmonic-photonic cavities may find wide applications in integrated opto-plasmonic devices for quantum information processing, nano-lasers, and sensing elements for surface-enhanced Raman scattering.

5. Summary and outlook

The field of hybrid cavity systems based on dielectric microcavities and plasmonic nano-particles or nano-antennas has made great progress over the past decades. This review has introduced the photonic crystal microcavities, surface plasmon resonances, and photonic-plasmonic hybrid microcavities from physics to applications. The hybrid microcavities play an important role in enhancing the light–matter interaction and their advantages are presented in Table 1. Compared with bare PhC microcavity, the hybrid microcavity based on PhC microcavity possesses higher figure of merit Q/V. For bare WGM microcavity and bare F-P microcavity, the figure of merit Q/V is lower than that of hybrid microcavity based on WGM microcavity and hybrid microcavity based on F-P microcavity respectively. Besides, the strength of light–matter interaction in hybrid microcavities is large enough to realize strong coupling, such as in hybrid microcavity based on PhC microcavity and hybrid microcavity based on F-P microcavity. Since topology has promoted the growth of photonics by

Table 1. The advantages of photonic-plasmonic hybrid microcavities.

Cavity type	Quality factor Q	Mode volume $V\ (\lambda/n)^3$	Figure of merit $Q/V\ (\lambda/n)^{-3}$	Strong coupling realization	Cooperativity parameter	Ref.
L3 PhC microcavity	2.3×10^5	0.73	3.2×10^5	No	–	[65]
WGM microcavity	10^4	10	10^3	No	–	[62]
F-P microcavity	3.4×10^3	0.44	7.7×10^3	No	–	[68]
Hybrid microcavity based on PhC microcavity	9.8×10^4	1.2×10^{-2}	8.4×10^6	Yes	6.4×10^5	[65]
Hybrid microcavity based on WGM microcavity	6.9×10^3	0.82	8.4×10^3	No	–	[62]
Hybrid microcavity based on F-P microcavity	980	9.6×10^{-4}	1.0×10^6	Yes	2.7×10^5	[68]

enabling its robustness, the physics and applications of topological photonic crystal microcavities, and topological hybrid microcavities have also been discussed, which provide robust platforms to study the coupling between light and matter. As is reported in previous works, the hybrid cavity systems indeed have great advantages in enhancing the light–matter interaction and are widely used in cavity quantum electrodynamics (cavity QED), nonlinear optics, quantum information processing, etc. In the coming years, the hybrid cavity systems still have a great potential in realizing strong light–matter interaction since they can own the advantages of both dielectric cavities and plasmonic cavities simultaneously.

However, there are also several challenges. One is the mastery of controlled coupling between the dielectric cavities and plasmonic cavities, which is determined by whether the plasmonic antennas can place onto the right position of dielectric cavities with high manipulation precision. Therefore, mature manipulation technology is critically important and novel approaches must be developed to overcome the drawbacks of self-assembly of hybrid cavities. Another one is the challenge to integrate the hybrid systems with molecules and quantum dots, which can indeed observe huge fluorescence enhancement or other physical phenomenon based on the platform of hybrid systems in experiments. If these issues have been addressed, hybrid cavity systems may find more applications in integrated optical devices for quantum information processing, nano-lasers, and sensing elements for surface-enhanced Raman scattering.

References

[1] Liu N, Gocalinska A, Justice J, Gity F, Povey I, McCarthy B, Pemble M, Pelucchi E, Wei H, Silien C, Xu H X and Corbett B 2016 *Nano Lett.* **16** 7822

[2] Mauranyapin N P, Madsen L S, Taylor M A, Waleed M and Bowen W P 2017 *Nat Photonics.* **11** 477

[3] Liang F, Guo Y Z, Hou S C and Quan Q M 2017 *Sci Adv.* **3** e1602991

[4] Yang D Q, Wang A Q, Chen J H, Yu X C, Lan C W, Ji Y F and Xiao Y F 2020 *Photonics Res.* **8** 497

[5] Jana S, Xu X Z, Klymchenko A, Reisch A and Pons T 2021 *ACS Nano.* **15** 1445

[6] Xu P, He X D, Wang J and Zhan M S 2010 *Opt. Lett.* **35** 2164

[7] Chen Y J, Zigo S and Raithel G 2014 *Phys Rev A.* **89** 063409

[8] Quy H Q, Tuan D Q, Thanh T D and Thang N M 2018 *Opt. Commun.* **427** 341

[9] Sesin P, Anguiano S, Bruchhausen A E, Lemaître A and Fainstein A 2021 *Phys. Rev. B.* **103** L081301

[10] Reithmaier J P, Sek G, Loffler A, Hofmann C, Kuhn S, Reitzenstein S, Keldysh L V, Kulakovskii V D, Reinecke T L and Forchel A 2004 *Nature* **432** 197

[11] Yoshie T, Scherer A, Hendrickson J, Khitrova G, Gibbs H M, Rupper G, Ell C, Shchekin O B and Deppe D G 2004 *Nature* **432** 200

[12] Faraon A, Fushman I, Englund D, Stoltz N, Petroff P and Vuckovic J 2008 *Nat. Phys.* **4** 859

[13] Nomura M, Kumagai N, Iwamoto S, Ota Y and Arakawa Y 2010 *Nat. Phys.* **6** 279

[14] van der Marel N, van Dishoeck E F, Bruderer S, Birnstiel T, Pinilla P, Dullemond C P, van Kempen T A, Schmalzl M, Brown J M, Herczeg G J, Mathews G S and Geers V 2013 *Science* **340** 1202

[15] Bose R, Cai T, Choudhury K R, Solomon G S and Waks E 2014 *Nat. Photon.* **8** 858

[16] Chow W W, Jahnke F and Gies C 2014 *Light Sci. Appl.* **3** e201

[17] Li J, Lin Y, Lu J F, Xu C X, Wang Y Y, Shi Z L and Dai J 2015 *ACS Nano.* **9** 6794

[18] Zhang W, Peng L, Liu J, Tang A, Hu J S, Yao J N and Zhao Y S 2016 *Adv. Mater.* **28** 4040

[19] Kreinberg S, Chow W W, Wolters J, Schneider C, Gies C, Jahnke F, Höfling S, Kamp M and Reitzenstein S 2017 *Light Sci. Appl.* **6** e17030

[20] Gong Y K, Wong S H, Bennett A J, Huffaker D L and Oh S S 2020 *ACS Photon.* **7** 2089

[21] Zhang J, Li J X, Tang S W, Fang Y F, Wang J, Huang G S, Liu R, Zheng L, Cui X G and Mei Y F 2015 *Sci. Rep.* **5** 15012

[22] Garaei M A, Saliminasab M, Nadgaran H and Moradian R 2017 *Plasmonics* **12** 1953

[23] Huang Q L and Cunningham B T 2019 *Nano Lett.* **19** 5297

[24] Xin K, Shi X F, Liu Y, Zhang Z M, Jia W J and Ma J 2020 *Opt. Express.* **28** 8734

[25] Vahala K J 2003 *Nature* **424** 839

[26] Yamamoto T, Pashkin Y A, Astafiev O, Nakamura Y and Tsai J S 2003 *Nature* **425** 941

[27] Akahane Y, Asano T, Song B S and Noda S 2005 *Opt. Express* **13** 1202

[28] Maeno K, Takahashi Y, Nakamura T, Asano T and Noda S 2017 *Opt. Express* **25** 367

[29] Asano T, Ochi Y, Takahashi Y, Kishimoto K and Noda S 2017 *Opt. Express* **25** 1769

[30] Asano T and Noda S 2018 *Opt. Express* **26** 32704

[31] Spillane S M, Kippenberg T J and Vahala K J 2002 *Nature* **415** 621

[32] Armani D K, Kippenberg T J, Spillane S M and Vahala K J 2003 *Nature* **421** 925

[33] Kippenberg T J, Spillane S M and Vahala K J 2004 *Phys. Rev. Lett.* **93** 83904

[34] Flatae A M, Burresi M, Zeng H, Nocentini S, Wiegele S, Parmeggiani C, Kalt H and Wiersma D 2015 *Light Sci. Appl.* **4** e282

[35] Chen Y L, Jin W L, Xiao Y F and Zhang X M 2016 *Phys. Rev. Appl.* **6** 044021

[36] Murphy R M J, Lei F, Ward J M, Yang Y and Chormaic S N 2017 *Opt. Express* **25** 13101

[37] Lippolis D, Wang L and Xiao Y F 2017 *Phys. Rev. E* **96** 12217

[38] Huang S H, Jiang X, Peng B, Janisch C, Cocking A, Özdemir Ş K, Liu Z and Yang L 2018 *Photonics Res.* **6** 346

[39] Gorodetsky M L, Savchenkov A A and Ilchenko V S 1996 *Opt. Lett.* **21** 453

[40] Vernooy D W, Ilchenko V S, Mabuchi H, Streed E W and Kimble H J 1997 *Opt. Lett.* **23** 247

[41] Burek M J, Chu Y W, Liddy M S Z, Patel P, Rochman J, Meesala S, Hong W, Quan Q M, Lukin M D and Lončar M 2014 *Nat. Commun.* **5** 5718

[42] Taverne M P C, Ho Y D, Zheng X, Chen L, Fang C N and Rarity J 2018 *Opt. Lett.* **43** 5202

[43] Caiyang W N, Jiang P, Qin Y, Mao S Q, Cao B, Gui F J and Yang H J 2019 *Opt. Express* **27** 4176
[44] Cheng W, Han Z, Du Y and Qin J 2019 *Opt. Express* **27** 16071
[45] Moczała-Dusanowska M, Dusanowski Ł, Iff O, Huber T, Kuhn S, Czyszanowski T, Schneider C and Höfling S 2020 *ACS Photon.* **7** 3474
[46] Asano T and Noda S 2018 *Opt. Express* **26** 32704
[47] Lin Y C, Chou S H and Hsueh W J 2020 *Sci. Rep.* **10** 1
[48] Barnes W L, Dereux A and Ebbesen T W 2003 *Nature* **424** 824
[49] Hutter E and Fendler J H 2004 *Adv. Mater.* **16** 1685
[50] Willets K A and Van Duyne R P 2007 *Annu. Rev. Phys. Chem.* **58** 267
[51] Khatua S, Paulo P M R, Yuan H, Gupta A, Zijlstra P and Orrit M 2014 *ACS Nano* **8** 4440
[52] Ayala-Orozco C, Liu J G, Knight M W, Wang Y, Day J K, Nordlander P and Halas N J 2014 *Nano Lett.* **14** 2926
[53] Pelton M 2015 *Nat. Photon.* **9** 427
[54] Chikkaraddy R, de Nijs B, Benz F, Barrow S J, Scherman O A, Rosta E, Demetriadou A, Fox P, Hess O and Baumberg J J 2016 *Nature* **535** 127
[55] Holsteen A L, Raza S, Fan P, Kik P G and Brongersma M L 2017 *Science* **358** 1407
[56] Kuttge M, Garcia De Abajo F J and Polman A 2010 *Nano Lett.* **10** 1537
[57] Russell K J, Liu T, Cui S Y and Hu E L 2012 *Nat. Photon.* **6** 459
[58] Chikkaraddy R, de Nijs B, Benz F, Barrow S J, Scherman O A, Rosta E, Demetriadou A, Fox P, Hess O and Baumberg J J 2016 *Nature* **535** 127
[59] Hoang T B, Akselrod G M and Mikkelsen M H 2015 *Nano Lett.* **16** 270
[60] Xiao Y F, Liu Y C, Li B B, Chen Y L, Li Y and Gong Q H 2012 *Phys. Rev. A* **85** 031805
[61] Liu Y C , Luan X S, Li H K, Gong Q H, Wong C W and Xiao Y F 2014 *Phys. Rev. Lett.* **112** 213602
[62] Doeleman H M, Verhagen E and Koenderink A F 2016 *ACS Photon.* **3** 1943
[63] Peng P, Liu Y C, Xu D, Cao Q T, Lu G W, Gong Q H and Xiao Y F 2017 *Phys. Rev. Lett.* **119** 233901
[64] Zhu G X and Liao Q G 2018 *Opt. Express* **26** 31391
[65] Zhang H Y, Liu Y C, Wang C Y, Zhang N E and Lu C C 2020 *Opt. Lett.* **45** 4794
[66] Cognée K G, Doeleman H M, Lalanne P and Koenderink A F 2019 *Light Sci. Appl.* **8** 115
[67] Barth M, Schietinger S, Fischer S, Becker J, Nusse N, Aichele T, Lochel B, Sonnichsen C and Benson O 2010 *Nano Lett.* **10** 891
[68] Gurlek B, Sandoghdar V and Martin-Cano D 2018 *ACS Photon.* **5** 456
[69] Conteduca D, Reardon C, Scullion M G, Dell' Olio F, Armenise M N, Krauss T F and Ciminelli 2017 *APL Photon.* **2** 086101
[70] Zhang T P, Callard S, Jamois C, Chevalier C, Feng D and Belarouci A 2014 *Nanotechnology* **25** 315201
[71] Conteduca D, Dell Olio F, Innone F, Ciminelli C and Armenise M N 2016 *Opt. Laser Technol.* **77** 151
[72] Franke S, Hughes S, Dezfouli M K, Kristensen P T, Busch K, Knorr A and Richter M 2019 *Phys. Rev. Lett.* **122** 213901
[73] Doeleman H M, Dieleman C D, Mennes C, Ehrler B and Koenderink A F 2020 *ACS Nano.* **14** 12027
[74] Gérard J, Sermage B, Gayral B, Legrand B, Costard E and Thierry-Mieg V 1998 *Phys. Rev. Lett.* **81** 1110
[75] Hood C J, Lynn T W, Doherty A C, Parkins A S and Kimble H J 2000 *Science* **287** 1447
[76] Qiao Q, Xia J, Lee C, and Zhou G 2018 *Micromachines-Basel* **9** 541
[77] Ward J and Benson O 2011 *Laser Photonics Rev.* **5** 553
[78] Youcef Mahmoud M, Bassou G, Taalbi A and Chekroun Z M 2012 *Opt. Commun.* **285** 368
[79] Liu L, Liao S, Xue W and Yue J 2020 *Opt. Express* **28** 6918
[80] Rokhsari H and Vahala K J 2004 *Phys. Rev. Lett.* **92** 253901
[81] Chow E, Grot A, Mirkarimi L W, Sigalas M and Girolami G 2004 *Opt. Lett.* **29** 1093
[82] Yang D Q and Zhang X 2019 *Opt. Commun.* **435** 11
[83] Kassa-Baghdouche L and Cassan E 2020 *Opt. Quant. Electron.* **52** 260
[84] Vollmer F, Arnold S and Keng D 2008 *Proc. Natl. Acad. Sci. USA* **105** 20701
[85] He L N, Özdemir Ş K, Zhu J G, Kim W and Yang L 2011 *Nat. Nanotechnol.* **6** 428
[86] Shao L B, Jiang X F, Yu X C, Li B B, Clements W R, Vollmer F, Wang W, Xiao Y F and Gong Q H 2013 *Adv. Mater.* **25** 5616
[87] Dong C H, He L, Xiao Y F, Gaddam V R, Ozdemir S K, Han Z F, Guo G C and Yang L 2009 *Appl. Phys. Lett.* **94** 231119
[88] Ioppolo T and Volkan Ötugen M 2007 *J. Opt. Soc. Am. B* **24** 2721
[89] Loncar M, Yoshie T and Scherer A 2002 *Appl. Phys. Lett.* **81** 2680
[90] Ee H S, Jeong K Y, Seo M K, Lee Y H and Park H G 2008 *Appl. Phys. Lett.* **93** 11104
[91] Nomura M, Ota Y, Kumagai N, Iwamoto S and Arakawa Y 2010 *Appl. Phys. Lett.* **97** 191108
[92] Athanasiou M, Smith R, Liu B and Wang T 2015 *Sci. Rep.* **4** 7250
[93] Guo J Q, Song G, Huang Y, Liang K, Wu F, Jiao R Z and Yu L 2021 *ACS Photon.* **8** 901
[94] Hennessy K, Badolato A, Winger M, Gerace D, Atatüre M, Gulde S, Fält S, Hu E L and Imamoğlu A 2007 *Nature* **445** 896
[95] Ota Y, Iwamoto S, Kumagai N and Arakawa Y 2011 *Phys. Rev. Lett.* **107** 233602
[96] Raimond J M, Brune M and Haroche S 2001 *Rev. Mod. Phys.* **73** 565
[97] Aram M H and Khorasani S 2015 *J. Mod. Phys.* **6** 1467
[98] Noda S and Baba T 2003 *Roadmap on Photonic Crystals* (Boston: Springer) p. 13
[99] Foresi J S, Villeneuve P R, Ferrera J, Thoen E R, Steinmeyer G, Fan S, Joannopoulos J D, Kimerling L C, Smith H I and Ippen E P 1997 *Nature* **390** 143
[100] Sekoguchi H, Takahashi Y, Asano T and Noda S 2014 *Opt. Express* **22** 916
[101] Asano T, Ochi Y, Takahashi Y, Kishimoto K and Noda S 2017 *Opt. Express* **25** 1769
[102] Asano T and Noda S 2018 *Opt. Express* **26** 32704
[103] Wang W H and Zhang N 2018 *Acta Phys. Sin.* **67** 247302 (in Chinese)
[104] Dousse A, Suffczyński J, Beveratos A, Krebs O, Lemaître A, Sagnes I, Bloch J, Voisin P and Senellart P 2010 *Nature* **466** 217
[105] Törmä P and Barnes W L 2014 *Rep. Prog. Phys.* **78** 13901
[106] Xu D, Xiong X, Lin W, Ren X F, Png C E, Guo G C, Gong Q H and Xiao Y F 2018 *Adv. Opt. Photon.* **10** 703
[107] Zhou Z K, Liu J F, Bao Y J, Wu L, Png C E, Wang X H and Qiu C W 2019 *Prog. Quant. Eletron.* **65** 1
[108] Genevet P, Tetienne J, Gatzogiannis E, Blanchard R, Kats M A, Scully M O and Capasso F 2010 *Nano Lett.* **10** 4880
[109] Harutyunyan H, Volpe G, Quidant R and Novotny L 2012 *Phys. Rev. Lett.* **108** 217403
[110] Yang X Y, Hu X Y, Yang H and Gong Q H 2017 *Nanophotonics* **6** 365
[111] Xie J Y, Niu X X, Hu X Y, Wang F F, Chai Z, Yang H and Gong Q H 2017 *Nanophotonics* **6** 1161
[112] Xu H F, Zhu Z M, Xue J C, Zhan Q Q, Zhou Z K and Wang X H 2021 *Photon. Res.* **9** 395
[113] Zengin G, Wersäll M, Nilsson S, Antosiewicz T J, Käll M and Shegai T 2015 *Phys. Rev. Lett.* **114** 157401
[114] Liu R M, Zhou Z K, Yu Y C, Zhang T W, Wang H, Liu G H, Wei Y M, Chen H J and Wang X H 2017 *Phys. Rev. Lett.* **118** 237401
[115] Wang B, Zeng X Z and Li Z Y 2020 *Photonics Res.* **8** 343
[116] Liu J N, Huang Q L, Liu K K, Singamaneni S and Cunningham B T 2017 *Nano Lett.* **17** 7569
[117] Zheng S B and Guo G C 2000 *Phys. Rev. Lett.* **85** 2392
[118] Mabuchi H and Doherty A C 2002 *Science* **298** 1372
[119] Duan L M and Kimble H J 2004 *Phys. Rev. Lett.* **92** 127902
[120] Miller R, Northup T E, Birnbaum K M, Boca A, Boozer A D and Kimble H J 2005 *J. Phys. B: At. Mol. Opt. Phys.* **38** S551
[121] Yao W, Liu R B and Sham L J 2005 *Phys. Rev. Lett.* **95** 30504
[122] Khitrova G, Gibbs H M, Kira M, Koch S W and Scherer A 2006 *Nat. Phys.* **2** 81
[123] Pellizzari T, Gardiner S A, Cirac J I and Zoller P 1995 *Phys. Rev. Lett.* **75** 3788
[124] Cirac J I, Zoller P, Kimble H J and Mabuchi H 1997 *Phys. Rev. Lett.* **78** 3221
[125] Shore B W and Knight P L 1993 *J. Mod. Opt.* **40** 1195
[126] Purcell E M 1946 *Phys. Rev.* **69** 681
[127] Ota Y, Katsumi R, Watanabe K, Iwamoto S and Arakawa Y 2018 *Commun. Phys.* **1** 86
[128] Han C, Lee M, Callard S, Seassal C and Jeon H 2019 *Light-Sci. Appl.* **8** 40
[129] Xie X, Zhang W X, He X W, Wu S Y, Dang J C, Peng K, Song F L, Yang L L, Ni H Q, Niu Z C, Wang C, Jin K J, Zhang X D and Xu X L 2020 *Laser Photonics Rev.* **14** 1900425
[130] Bandres M A, Wittek S, Harari G, Parto M, Ren J, Segev M, Christodoulides D N and Khajavikhan M 2018 *Science* **359** eaar4005

[131] Zhang W X, Xie X, Hao H M, Dang J C, Xiao S, Shi S S, Ni H Q, Niu Z C, Wang C, Jin K J, Zhang X D and Xu X L 2020 *Light-Sci. Appl.* **9** 109

[132] Ao Y T, Hu X Y, You Y L, Lu C C, Fu Y L, Wang X Y and Gong Q H 2020 *Phys. Rev. Lett.* **125** 013902

[133] Lu C C, Wang C Y, Xiao M, Zhang Z Q and C T Chan 2021 *Phys. Rev. Lett.* **126** 113902

[134] Xie B Y, Wang H F, Wang H X, Zhu X Y, Jiang J H, Lu M H and Chen Y F 2018 *Phys. Rev. B* **98** 205147

[135] Chen X D, Deng W M, Shi F L, Zhao F L, Chen M and Dong J W 2019 *Phys. Rev. Lett.* **122** 233902

[136] Chen Y F, Meng F, Li G Y and Huang X D 2019 *Acta Mater.* **164** 377

[137] Ota Y, Liu F, Katsumi R, Watanabe K and Wakabayashi K 2019 *Optica* **6** 786

[138] Kim M and Rho J 2020 *Nanophotonics* **9** 3227

[139] Qian Z, Li Z, Hao H, Shan L, Zhang Q, Dong J, Gong Q and Gu Y 2021 *Phys. Rev. Lett.* **126** 23901

[140] Zhang H Y, Zheng Y J, Yu Z M, Hu X Y and Lu C C 2021 *J. Opt.* (Accepted)